



Characterization of a novel deep-intronic variant in *DYNC2H1* identified by whole-exome sequencing in a patient with a lethal form of a short-rib thoracic dysplasia type III

Muqsit Buchh,^{1,4} Patrick J. Gillespie,^{1,4} Kayla Treat,^{1,2,3} Marco A. Abreu,¹ Tae-Hwi Linus Schwantes-An,^{1,2,3} Benjamin M. Helm,^{1,2,3} Fang Fang,¹ Xiaoling Xuei,¹ Lili Mantcheva,¹ Kristen R. Suhrie,¹ Brett H. Graham,¹ Erin Conboy,^{1,2,3,4} and Francesco Vettrini^{1,2,3,4}

¹Indiana University School of Medicine, Indianapolis, Indiana 46202, USA; ²Department of Medical and Molecular Genetics, Indiana University School of Medicine, Indianapolis, Indiana 46202, USA; ³Undiagnosed Rare Disease Clinic (URDC), Indiana University School of Medicine, Indianapolis, Indiana 46202, USA

Abstract Biallelic pathogenic variants in *DYNC2H1* are the cause of short-rib thoracic dysplasia type III with or without polydactyly (OMIM #613091), a skeletal ciliopathy characterized by thoracic hypoplasia due to short ribs. In this report, we review the case of a patient who was admitted to the Neonatal Intensive Care Unit (NICU) of Indiana University Health (IUH) for respiratory support after experiencing respiratory distress secondary to a small, narrow chest causing restrictive lung disease. Additional phenotypic features include postaxial polydactyly, short proximal long bones, and ambiguous genitalia were noted. Exome sequencing (ES) revealed a maternally inherited likely pathogenic variant c.10322C > T p.(Leu3448Pro) in the *DYNC2H1* gene. However, there was no variant found on the paternal allele. Microarray analysis to detect deletion or duplication in *DYNC2H1* was normal. Therefore, there was insufficient evidence to establish a molecular diagnosis. To further explore the data and perform additional investigations, the patient was subsequently enrolled in the Undiagnosed Rare Disease Clinic (URDC) at Indiana University School of Medicine (IUSM). The investigators at the URDC performed a reanalysis of the ES raw data, which revealed a paternally inherited *DYNC2H1* deep-intronic variant c.10606-14A > G predicted to create a strong cryptic acceptor splice site. Additionally, the RNA sequencing of fibroblasts demonstrated partial intron retention predicted to cause a premature stop codon and nonsense-mediated mRNA decay (NMD). Droplet digital RT-PCR (RT-ddPCR) showed a drastic reduction by 74% of *DYNC2H1* mRNA levels. As a result, the intronic variant was subsequently reclassified as likely pathogenic resulting in a definitive clinical and genetic diagnosis for this patient. Reanalysis of ES and fibroblast mRNA experiments confirmed the pathogenicity of the splicing variants to supplement critical information not revealed in original ES or CMA reports. The NICU and URDC collaboration ended the diagnostic odyssey for this family; furthermore, its importance is emphasized by the possibility of prenatally diagnosing the mother's current pregnancy.

Correspondence:
fvetrini@iu.edu; econboy@iu.edu

© 2022 Buchh et al. This article is distributed under the terms of the Creative Commons Attribution-NonCommercial License, which permits reuse and redistribution, except for commercial purposes, provided that the original author and source are credited.

Ontology terms: ambiguous genitalia, male; bilateral postaxial polydactyly; deformed rib cage; hydronephrosis; lethal skeletal dysplasia; patent foramen ovale; rhizomelic arm shortening

Published by Cold Spring Harbor Laboratory Press

doi:10.1101/mcs.a006254

[Supplemental material is available for this article.]

⁴These authors contributed equally to this work.

INTRODUCTION

Short-rib thoracic dysplasia (SRTD) with or without polydactyly is a group of autosomal recessive skeletal ciliopathies characterized by a constricted thoracic cage, short ribs, shortened tubular bones, and an acetabular roof with a “trident” appearance. Some forms of SRTD are lethal in the neonatal period because of respiratory insufficiency secondary to a severely restricted thoracic cage, whereas others are compatible with life (Huber and Cormier-Daire 2012). There are more than 20 genes described responsible for different forms of SRTD, which present with significant overlap and variability, and most of them encode for ciliary proteins involved in intraflagellar transport (Huber and Cormier-Daire 2012; Hammarsjö et al. 2021). The most commonly mutated gene in SRTD is *DYNC2H1*, encoding the central ATPase subunit of IFT dynein-2 complex heavy chain, which is necessary for its proper functioning (Schmidts et al. 2013a). Dyneins are ATP-driven motor complex proteins that engage in retrograde transport of cellular cargo along eukaryotic cilia and flagella axonemes (Roberts 2018). Malfunction of the dynein-2 proteins can lead to a broad family of diseases: short-rib polydactyly syndrome, Jeune asphyxiating thoracic dysplasia, Mainzer–Saldino syndrome, and Ellis–van Creveld syndrome (Schmidts and Mitchison 2018). Symptoms of short-rib thoracic dysplasia type III (SRTD3) include shortened ribs, narrowed thorax, and significantly shortened tubular bones. Other characteristics, radiological findings, and malformations can affect the face, gastrointestinal tract, urogenital tract, brain, or heart (Dagoneau et al. 2009). Patients with a clinical diagnosis of SRTD3 are identified by carrying biallelic pathogenic or likely pathogenic variants in the *DYNC2H1* gene (Merrill et al. 2009).

Exome sequencing (ES) is used to analyze ~2% of the genome including exons, portions of introns, intergenic regions, untranslated regions, and intron–exon boundaries (Guo et al. 2012). Variant detection is limited to a small number of nucleotides within the noncoding regions, which includes intron–exon boundary, 5'/3' UTR, and part of promoters. Pathogenic variants in introns outside of the sequenced regions or outside the regions called by the diagnostic laboratory can remain undetected or unreported. These variants can be discovered through whole genome sequencing (GS) or, in many instances, by reanalyzing the ES raw data. However, in absence of functional studies, variants predicted to affect splicing outside the conserved GT-AG canonical sites, even when supported by additional evidence (segregation patterns, specific gene–disease association, rarity in normal population databases), can still pose an interpretive challenge to clinical geneticists and laboratorians. Multiple independent studies have shown that the utilization of RNA sequencing (RNA-seq) to supplement DNA analysis (ES/GS) in rare disease investigations increased the diagnostic yields ranging from 7% to 36% (Lee et al. 2014; Gonorazky et al. 2019; Rentas et al. 2020; Murdock et al. 2021; Yépez et al. 2021).

In this report, we present the case of a patient admitted to the Neonatal Intensive Care Unit (NICU) of Indiana University Health for respiratory support presenting with postaxial polydactyly, short ribs, short thorax, rhizomelia, hydronephrosis, and cardiac malformations. A molecular diagnosis was not initially made from the clinical testing because prior ES revealed only one likely pathogenic missense variant in the *DYNC2H1* gene inherited from the mother. The subsequent enrollment of the patient in the Undiagnosed Rare Disease Clinic (URDC) allowed further research investigations, including reanalysis of ES, RNA-seq, and gene expression analysis, that ultimately yielded an unequivocal definitive molecular diagnosis.

RESULTS

Clinical Presentation of the Case

The mother of the patient was a G6P3022 27-yr-old female; the parents were nonconsanguineous. The patient had two older healthy siblings, and one brother that died because

of complications of croup, and two first trimester miscarriages at 5 wk and 7 wk. The first indication of abnormal growth in this patient was ultrasound findings at 19 wk and 1 d showing abnormally short upper and lower extremity length. An ultrasound was performed at 20 wk and 6 d to quantify shortening of bones, intrauterine growth restriction, polydactyly, abdominal, and genital abnormalities (not shown). Ultrasound measurements yielded a femur length:foot length ratio of 0.76, with skeletal dysplasia typically indicated in ratios below 1.00 (Fig. 1; Campbell et al. 1988). A chest circumference:abdominal circumference ratio of 0.71 was calculated, with a ratio of <0.6 being indicative of lethality (Krakow et al. 2009). Taken together, this data suggested a nonlethal form of skeletal dysplasia, and the family was informed that possible diagnoses include skeletal ciliopathies and short-rib polydactyly syndrome. The patient was born at term with significant cyanosis and O₂ saturation levels between 55% and 65%; he was emergently transferred to the NICU for respiratory support. A skeletal survey completed at 1 d of age revealed a narrow thorax with mildly shortened ribs, shortened metacarpal and metatarsal bones, and abnormal lucency at the distal metaphyses of all the long bones of the upper and lower extremities (Fig. 1). Initial general exam found a small, bell-shaped chest, rhizomelic shortening of all extremities, polydactyly of the hand, brachydactyly of all digits, syndactyly, and significant micropenis without discernible foreskin (Fig. 2). In addition, he was affected by abnormal aortic morphology with a patent ductus arteriosus, a patent foramen ovale, cervical spinal stenosis, and hydronephrosis. Trio-based ES initial analysis was reported from GeneDx 1 mo postnatally. A maternally inherited, heterozygous c.10322T > C; p.Leu3448Pro variant in the *DYNC2H1*

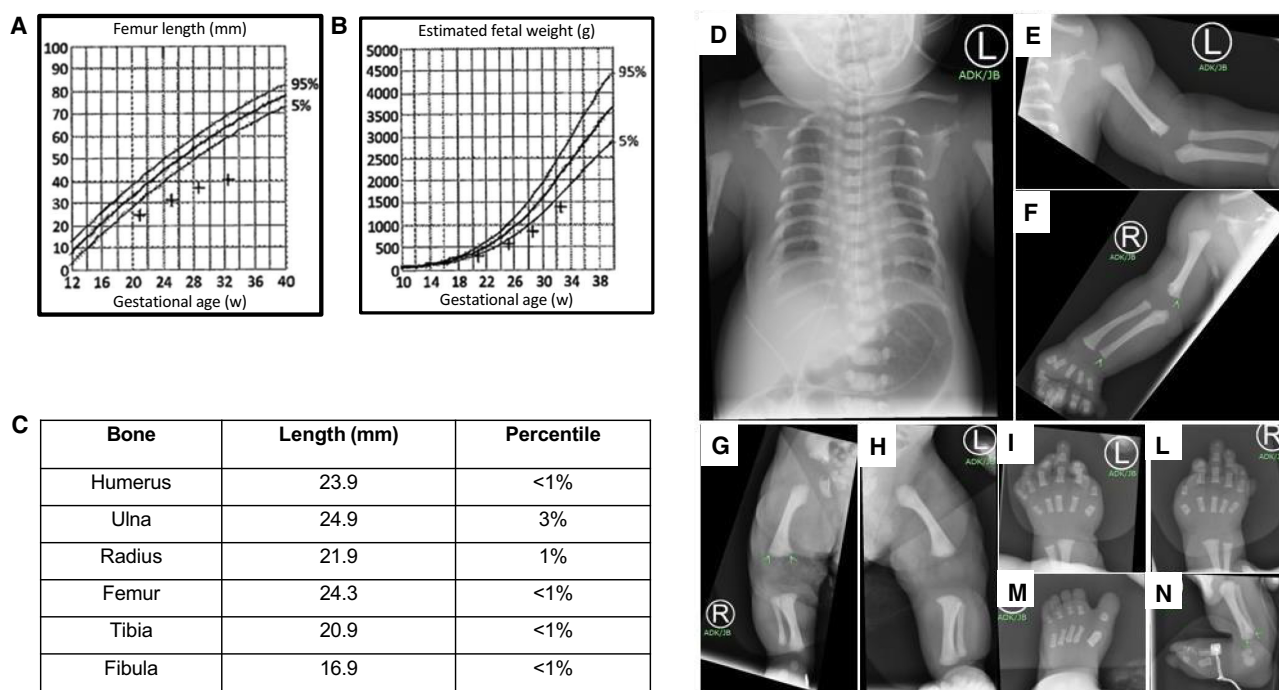


Figure 1. Patient prenatal characteristics. (A) Longitudinal femur length as a function of gestational age demonstrates severe shortened bones of the extremity. (B) Longitudinal fetal weight plotted as a function of gestational age compared to fifth percentile and 95th percentile fetuses at the estimated age. At 20 wk + 6 d, the patient's weight was in the second percentile. (C) Length of bones with percentile comparison to fetuses of similar age. (D) Narrow thorax with mildly shortened ribs. (E–H) Abnormal lucency at the distal metaphyses of all the long bones of the upper and lower extremities. (I, L) Postaxial polydactyly of the hands, bilaterally. (M, N) Shortened metacarpal and (M, N) metatarsal bones.



Figure 2. Patient postnatal characteristics. (A) Patient's left hand with postaxial polydactyly, proximally placed thumbs, and 5–6 finger syndactyly. (B) Patient's right hand with postaxial polydactyly and a hypoplastic sixth digit. (C) Small, bell-shaped chest. Rhizomelic shortening in all extremities. Brachydactyly of toes, 2–3 toe syndactyly bilaterally.

gene (NM_001377) was discovered. Although this had already been reported as a likely pathogenic variant by multiple studies (Table 1; Schmidts et al. 2013b; Stark et al. 2017; Dillon et al. 2018; Doornbos et al. 2021), initial ES analysis failed to reach a molecular diagnosis as only one heterozygous variant was found. The c.10322T > G p. (Leu3448Pro) variant is highly conserved during evolution, absent from control population databases, located in the ATP-binding dynein motor region domain D5, and predicted to be deleterious by multiple *in silico* predictive tools (ClinVar accession number VCV000369661.8) (Table 1). A chromosomal microarray (CMA) targeted to the *DYNC2H1* gene was performed using a blood sample and was negative for complete or partial deletion or duplication at exon-level resolution. The patient required gradually increasing continuous positive airway pressure (CPAP) therapy because of worsening respiratory distress, tachypnea, and desaturation events. Unfortunately, the patient was compassionately extubated at 2 months of age before sufficient evidence was garnered to generate a molecular and genetic diagnosis.

ES Reanalysis, RNA Studies, and Variant Reclassification

The family subsequently enrolled the patient in the URDC at the Indiana University School of Medicine (IUSM) because of failure to reach a molecular diagnosis and suspicion that a second variant was missed on ES. Reanalysis performed on raw data obtained from GeneDx revealed a novel deep-intronic c.10606-14A > G heterozygous variant inherited from father in the *DYNC2H1* gene (NM_001377), absent from gnomAD, which had the potential to confirm the diagnosis of SRTD3 (Table 1). *In silico* analysis predicted that *DYNC2H1* c.10606-14A > G introduced a novel strong acceptor splice site (Table 1; Fig. 3).

To determine the direct impact on splicing, RNA-seq analysis was performed using patient-derived fibroblasts. This showed that the intronic change activated a cryptic AG dinucleotide outcompeting the canonical acceptor site and causing the inclusion of additional 13 nt into exon 70 (r.10605_10606ins10606-14_10606-1) leading to a premature

Table 1. Variant table

Gene	Chromosome	HGVS DNA reference	HGVS protein reference	Predicted effect	In silico predictions	Genotype	ClinVar ID	Pathogenicity	Parent of origin
DYNC2H1 (NM_001080463.2)	GRCh37: Chr 11: 103126259T > C	c.10322T > C	p.(Leu3448Pro)	Missense substitution	PolyPhen-2: damaging, SIFT: damaging, MutationTaster: disease-causing, LRT: damaging, DANN: 0.998, REVEL: 0.824	Heterozygous	SCV002526657.1	Likely pathogenic	Maternal
DYNC2H1 (NM_001080463.2)	GRCh37: Chr 11: 103130603A > G	c.10606-14A > G	p.?	Splicing alteration	Splice AI, DS AG 0.7, ASSP, Alt 3.4, Ref 4.5, IntSplice ver1.1: abnormal	Heterozygous	SCV002513123.1	Likely pathogenic	Paternal

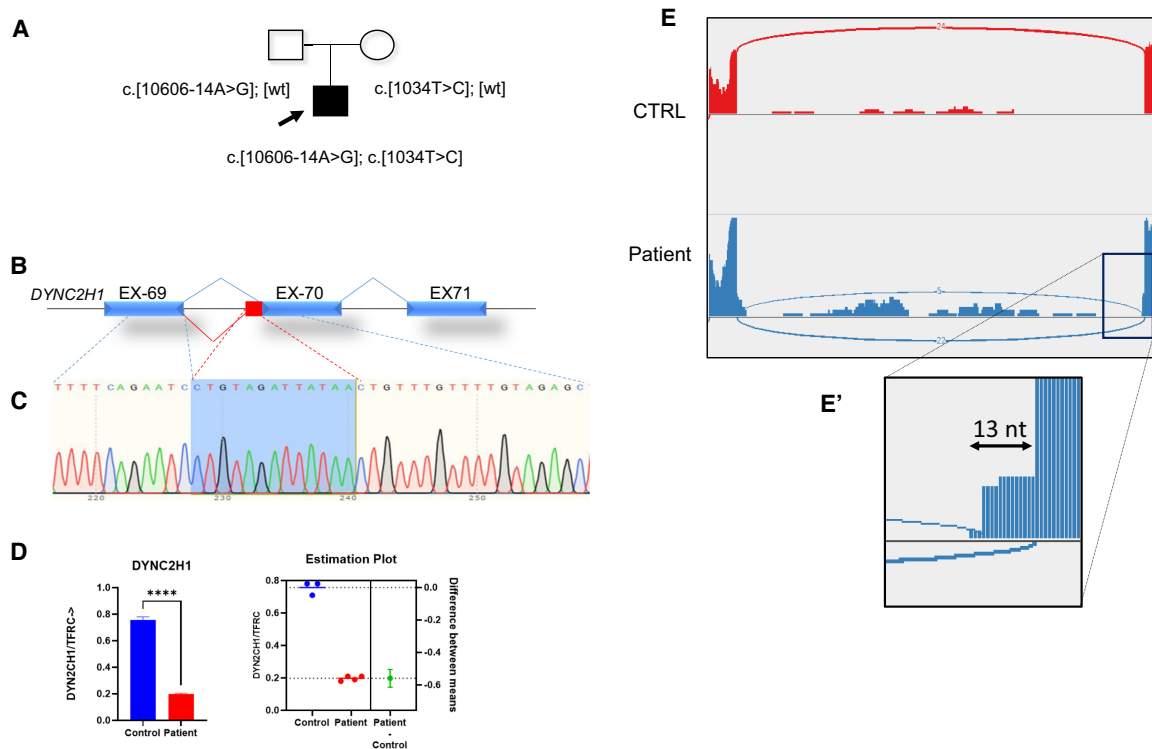


Figure 3. Characterization of c.10606-14A > G variant in *DYNC2H1*. (A) Pedigree of the family and segregation of the *DYNC2H1* variants. (B) Schematic representation of the genomic region encompassing exons 69–71 indicating the normal splice (top) and the alternative splicing (in red) showing abnormal intron retention (bottom). The red bar corresponds to the intronic region of 13 bp retained into the exon 70 when the cryptic splice site is activated. (C) Sequence of exon 69, intron retention, exon 70 in the cDNA sequence representative of 7/37 bacterial clones. (D) Droplet digital polymerase chain reaction (ddPCR) analysis of *DYNC2H1* mRNA expression in cDNA derived from patient- and control-derived fibroblasts. Statistical analysis (two-tailed, unpaired t-test) demonstrated a significant difference in the normalized expression level of *DYNC2H1* between the patient of interest and the control with a *P*-value of <0.0001. There is a 74% reduction in the amount of *DYNC2H1* expressed in the patient compared to the control. (E) Sashimi plot of *DYNC2H1* exons 69–70 showing the alternative splicing junction caused by the cryptic splice site activation. The difference between wild-type and mutant reads (*n* = 5) in the control (*n* = 22) could be explained by nonsense-mediated decay (NMD). (E') Magnification of the affected splice junction between intron 69 and exon 70, showing the 13-nt intronic retention caused by the mutation.

stop codon c.10605_10606ins13; p.Phe3537* (Fig. 3). Moreover, RNA obtained from patient-derived fibroblast cultures was subjected to reverse transcription-polymerase chain reaction (RT-PCR) by using specific primers designed around exons 69–72 and the product was subcloned and into pCR4 TOPO cloning, subsequently analyzed by Sanger sequencing. The results showed that seven of the 37 (19%) isolated bacterial clones retained the 13-nt intronic region into exon 70 (Fig. 3). To assess the effect of the c.10606-14A > G on *DYNC2H1* mRNA levels, we analyzed the expression profile by quantitative droplet digital PCR (ddPCR) analysis of *DYNC2H1* mRNA expression in cDNA derived from patient- and control-derived fibroblasts. Compared with the healthy control, the *DYNC2H1* mRNA levels in the patient were reduced by 74%, suggesting nonsense-mediated mRNA degradation (NMD) mechanism (Fig. 3).

Using the American College of Medical Genetics and Genomics (ACMG) guidelines (Richards et al. 2015), because multiple lines of computational evidence supported the

deleterious effect due to alternative splicing (PP3), the patient's highly specific phenotype with a single genetic etiology (PP4), and a detrimental effect observed by multiple RNA studies (PS3), the criteria for likely pathogenic variant (one strong, one moderate, and two supporting) were met. This information was sent to GeneDx and the intronic variant was reclassified and reported back to the family as likely pathogenic.

DISCUSSION

Annually, 10%–14% of newborns require care in a NICU following birth (Braun et al. 2020). In NICUs such as those at Riley Hospital for Children at Indiana University Health, published data, as well as internal data, indicate that as many as 30%–50% of NICU patients have signs or symptoms of a genetic disorder (Hagen et al. 2022). With conventional ES or GS, the diagnostic yield is reported to be 30%–50%, with most patients that achieve a diagnostic result experiencing a significant change in their medical care (Kingsmore et al. 2019; Dimmock et al. 2020, 2021; Maron et al. 2021). Achieving definitive answers for patients with signs or symptoms of a genetic diagnosis after receiving a nondiagnostic ES/GS test result poses a challenge for NICUs across the country and worldwide. The capability to explore uncharacterized regions of the genome, including potential noncoding regions amenable to RNA-seq analysis or other variant identification methods, is needed across a different spectrum of disorders and clinical settings. We described the case of a NICU patient with a lethal form of SRTD for whom the integration of ES reanalysis, RNA-seq, and expression analysis resulted in a definitive diagnosis, demonstrating the benefits of integrating research genome and RNA analysis beyond the initial clinical report to resolve the diagnostic uncertainty. The raw exome sequencing data proved to be a productive tool in finding a previously unidentified deep-intronic variant c.10606-14A > G in *DYNC2H1*. Deep-intronic splice variants are usually not identified in routine diagnostics because of its focus on protein-coding regions. This variant was not reported by the commercial diagnostic laboratory as it lies beyond their reporting criteria, based on their CAP/CLIA validation. However, multiple *in silico* tools predicted a detrimental effect on splicing by activating a strong cryptic acceptor splice site (ss) that outcompetes the natural acceptor site. Previous studies have shown that the distance between the cryptic 3' ss and the authentic 3' ss is critical for its activation. When the upstream cryptic splice site is <21 nt apart from the canonical 3' ss, the cryptic 3' ss is preferentially used (Wieringa et al. 1984; Chua and Reed 2001; Tavanez et al. 2012). Subsequent RNA studies performed on cultured fibroblasts obtained by skin biopsy revealed that 13 intronic nucleotides are retained within the exon 70 causing frameshift and a drastic reduction of mRNA levels, indicating NMD as the most plausible pathogenic mechanism.

In this case, the possibility of reanalyzing the ES provided the potential diagnosis which allowed for the omission of performing additional GS, yet another genetic test for the family to consent to. Future cases may be solved in a similar manner as it allows for variant discovery without waiting several weeks for additional results. However, because SRTD3 can also be caused by deep-intronic variants (Hammarsjö et al. 2021), often beyond the sensitivity of ES, in cases in which ES reanalysis is negative, GS is the reliable next step.

RNA-seq served a critical role in confirming the potential diagnosis by revealing the effect of the alteration and prompting additional RT-ddPCR experiments. As the tool of choice in determining pathogenicity of splicing variants, RNA sequencing has greatly improved in efficacy and applicability since its birth almost two decades ago (Stark et al. 2017). Patient-derived fibroblasts specifically have been demonstrated in this case report to be successful in identifying differential mRNA splicing. In addition, RNA sequencing of fibroblasts may even be better at detecting alterations of clinically relevant gene protein products than whole blood (Murdock et al. 2021). Whereas in this case fibroblasts were the only sample option

as they were collected postmortem, skin cells may be the preferable source of RNA in the future for all patients as suggested by recent studies (Murdock et al. 2021).

In summary, the reanalysis of ES, analysis of RNA sequencing, and further RNA studies confirmed the suspected genetic cause of disease in the NICU patient in this report. The detection and reclassification of the c.10606-14A>G variant in the *DYNC2H1* gene from variant of uncertain significance to likely pathogenic allowed for the confirmed diagnosis of short-rib thoracic dysplasia type III. The reclassification to likely pathogenic also expands the genotype of short-rib thoracic dysplasia type III, as this is a novel gene variant.

In this case report, we demonstrated the importance of two essential components in providing the definitive diagnosis of the suspected SRTD III in a newborn; first, the utilization of research-based ES reanalysis and RNA functional studies and, second, the valuable collaboration between the NICU and the URDC.

As evidenced by the case of this patient, time is essential in reaching a diagnosis. Although unlikely to change this particular patient's outcome, a direct, streamlined collaboration between the NICU and URDC would allow for reducing unnecessary diagnostic testing and the anguish of a difficult decision to withdraw care without a definitive diagnosis. There is evidence that ES and GS can inform clinical as well as reproductive decision making in care for pediatric patients, especially for those who have intellectual disability or congenital anomalies (Malinowski et al. 2020). Specifically for this case, the discovery of the paternally inherited, likely pathogenic variant in this family, which could affect future pregnancies, was communicated through a genetic counseling discussion. The family was informed of the 25% recurrence risk with each pregnancy and of the availability of prenatal testing and diagnosis for the condition, and this result will allow future preimplantation and prenatal genetic testing/diagnosis.

The certainty of a clinical diagnosis can provide direction of care for physicians and expectations of prognosis for the patient and family—both of which are essential tools in determining the best possible outcome for the patients. Such information could contribute to minimizing distress during difficult decisions. However, when initial results from ES and GS fail to yield a diagnosis, families are left with few answers. As presented above, the clinical exome alone may not be sufficient when a deep-intronic variant is the cause of the condition. The use of research-based ES reanalysis and RNA-seq followed by RT-qPCR analysis resulted in a higher diagnostic yield, implying that a formal multi-omics approach collaboration between the NICU and the URDC can help resolve the diagnostic mysteries of other unsolved cases, resulting in better outcomes for patients and their families. Future collaboration between the NICU and the URDC can direct families to clinical care specialists and geneticists dedicated to finding answers whenever possible.

METHODS

Genetic Testing and Variant Interpretation

Genomic DNA was extracted from the peripheral blood of the proband and his parents. Initial trio-based whole-exome sequencing (WES) analysis and Sanger sequencing was performed by GeneDx (please refer to Supplemental Table S1 in Supplemental Material for sequencing coverage information). Genomic DNA from the specimen was enriched for coding regions and splice site junctions for most genes on the human genome, sequenced on an Illumina platform, and then filtered and analyzed using their custom analysis tool. Variant reanalysis was performed using EMEDGENE analytical pipeline (<https://iuhealth.emedgene.com/>) and manually. Sequence variants were checked with population databases gnomAD (<http://gnomad.broadinstitute.org/>) and evaluated using Splice-AI, NN-splice, PolyPhen-2, MutationTaster, REVEL, DANN, LRT, and SIFT. Variant pathogenicity was interpreted according to the ACMG guidelines (Richards et al. 2015).

RNA Extraction and cDNA Analysis

Fibroblasts were isolated from the patient by skin biopsy and cell cultures were established. Total RNA was extracted from the fibroblast culture, and cDNA was reverse-transcribed from the RNA (ReliaPrep RNA Cell Miniprep System Promega Z6010). CDNA was subcloned into pCR4 TOPO (TOPO TA Cloning Kit; ThermoFisher 450071) and the plasmid was transformed into OmniMax2 T1R bacteria (ThermoFisher C854003). Bacteria were plated on kanamycin (50 mg/mL) plates, and then incubated overnight. Colonies were isolated using blue/white screening, cultured in LB broth (ampicillin 50 mg/mL) overnight. DNA was extracted from each clone, quantitated, and submitted for Sanger sequencing. Sequencing runs were compared to mammalian reference NG 016423. Digital PCR was performed to analyze expression of the *DYN2CH1* gene in the patient compared to a control. Briefly, the Applied Biosystems QuantStudio Absolute Q digital PCR system (Applied Biosystems A52864) was used to detect the amount of expressed *DYNC2H1* in fibroblasts derived from both the patient and an unaffected control. Absolute Q 1-Step RT-dPCR master mix (4×) (Absolute Q A55146) and total RNA (11.25 ng from the unaffected control or 72.5 ng RNA from the patient) isolated from fibroblasts were combined with duplexed TaqMan assays for *DYNC2H1* (ThermoFisher Assay ID Hs00300261_m1 (VIC)) and *TFRC* (ThermoFisher Assay ID Hs00951083_m1 (FAM)) (normalizing control). Three technical replicates were performed for the control sample, and four technical replicates were performed for the patient sample. Statistical analysis (two-tailed, unpaired *t*-test) demonstrated a significant difference in the normalized expression level of *DYNC2H1* between the patient of interest and the control with a *P*-value of <0.0001. There is a 74% reduction in the amount of *DYNC2H1* expressed in the patient compared to the control.

RNA Sequencing

Total RNA was first evaluated for its quantity, and quality, using Agilent Bioanalyzer 2100. For RNA quality, a RIN number of 7 or higher is desired. One hundred nanograms of total RNA was used. The cDNA library preparation included mRNA purification/enrichment, RNA fragmentation, cDNA synthesis, ligation of index adaptors, and amplification, following the KAPA mRNA Hyper Prep Kit Technical Data Sheet, KR1352 – v4.17 (Roche Corporate). Globin mRNAs were depleted using QIAseq FastSelect Globin Removal Kit after fragmentation of enriched mRNA, following the protocol of QIAseq FastSelect Handbook, June 2021 (QIAGEN). Each resulting indexed library was quantified and its quality accessed by Qubit and Agilent TapStation 4200, and multiple libraries were pooled in equal molarity. The pooled libraries were then denatured, and neutralized, before loading to NovaSeq 6000 sequencer at 300 pM final concentration for 100-bp paired-end sequencing (Illumina, Inc.). Approximately 30–40 million reads per library were generated. A Phred quality score (Q score) was used to measure the quality of sequencing. More than 90% of the sequencing reads reached Q30 (99.9% base call accuracy).

ADDITIONAL INFORMATION

Data Deposition and Access

The *DYNC2H1* variant and our interpretation have been submitted to ClinVar (<https://www.ncbi.nlm.nih.gov/clinvar/>) by GeneDX under the accession number SCV002513123.

Ethics Statement

The research project used medical health information and specimens that had been collected as part of an ongoing research study at the Undiagnosed Rare Disease Clinic at Indiana

University. Written informed consent was obtained from both parents for the collection, re-search use, and storage of the specimens according to the approved protocol by the Indiana University Institutional Review Board (IRB# 2005902680).

Acknowledgments

We extend our deep appreciation to the patient and his family for participating in this study. WES was performed by GeneDx. We thank Lili Mantcheva for helping with the IRB requirements. We thank Angela Reese for helping with fibroblast cultures.

Author Contributions

F.V. and E.C. proposed the meaning and concept of the study and designed the plan for the case. M.B., P.J.G., L.M., K.T., K.R.S., M.A.A., T-H.L.S-A., B.M.H., B.H.G., E.C., and F.V. made contributions to data collection and analysis. All of the authors read and approved the final manuscript to be published and agreed to be responsible for the accuracy of the data and details.

Competing Interest Statement

The authors have declared no competing interest.

Received October 21, 2022;
accepted in revised form
November 21, 2022.

Funding

This study is funded in part by the Indiana University Grand Challenge Precision Health Initiative.

REFERENCES

- Braun D, Braun E, Chiu V, Burgos AE, Gupta M, Volodarskiy M, Getahun D. 2020. Trends in neonatal intensive care unit utilization in a large integrated health care system. *JAMA Netw Open* **3**: e205239. doi:10.1001/jamanetworkopen.2020.5239
- Campbell J, Henderson A, Campbell S. 1988. The fetal femur/foot length ratio: a new parameter to assess dysplastic limb reduction. *Obstet Gynecol* **72**: 181–184.
- Chua K, Reed R. 2001. An upstream AG determines whether a downstream AG is selected during catalytic step II of splicing. *Mol Cell Biol* **21**: 1509–1514. doi:10.1128/MCB.21.5.1509-1514.2001
- Dagoneau N, Goulet M, Geneviève D, Sznajder Y, Martinovic J, Smithson S, Huber C, Baujat G, Flori E, Tecco L, et al. 2009. *DYNC2H1* mutations cause asphyxiating thoracic dystrophy and short rib-polydactyly syndrome, type III. *Am J Hum Genet* **84**: 706–711. doi:10.1016/j.ajhg.2009.04.016
- Dillon OJ, Lunke S, Stark Z, Yeung A, Thorne N; Melbourne Genomics Health Alliance, Gaff C, White SM, Tan TY. 2018. Exome sequencing has higher diagnostic yield compared to simulated disease-specific panels in children with suspected monogenic disorders. *Eur J Hum Genet* **26**: 644–651. doi:10.1038/s41431-018-0099-1
- Dimmock DP, Clark MM, Gaughran M, Cakici JA, Caylor SA, Clarke C, Feddock M, Chowdhury S, Salz L, Cheung C, et al. 2020. An RCT of rapid genomic sequencing among seriously ill infants results in high clinical utility, changes in management, and low perceived harm. *Am J Hum Genet* **107**: 942–952. doi:10.1016/j.ajhg.2020.10.003
- Dimmock D, Caylor S, Waldman B, Benson W, Ashburner C, Carmichael JL, Carroll J, Cham E, Chowdhury S, Cleary J, et al. 2021. Project Baby Bear: rapid precision care incorporating rWGS in 5 California children's hospitals demonstrates improved clinical outcomes and reduced costs of care. *Am J Hum Genet* **108**: 1231–1238. doi:10.1016/j.ajhg.2021.05.008
- Doombos C, van Beek R, Bongers EMHF, Lugtenberg D, Klaren PHM, Vissers LELM, Roepman R, Oud MM. 2021. Cell-based assay for ciliopathy patients to improve accurate diagnosis using ALPACA. *Eur J Hum Genet* **29**: 1677–1689. doi:10.1038/s41431-021-00907-9
- Gonorazky HD, Naumenko S, Ramani AK, Nelakuditi V, Mashouri P, Wang P, Kao D, et al. 2019. Expanding the boundaries of RNA sequencing as a diagnostic tool for rare Mendelian disease. *Am J Hum Genet* **104**: 1007. doi:10.1016/j.ajhg.2019.04.004
- Guo Y, Long J, He J, Li C, Cai Q, Shu XO, Zheng W, Li C. 2012. Exome sequencing generates high quality data in non-target regions. *BMC Genomics* **13**: 194. doi:10.1186/1471-2164-13-194
- Hagen L, Khattar D, Whitehead K, He H, Swarr DT, Suhrie K. 2022. Detection and impact of genetic disease in a level IV neonatal intensive care unit. *J Perinatol* **42**: 580–588. doi:10.1038/s41372-022-01338-0

- Hammarsjö A, Pettersson M, Chitayat D, Handa A, Anderlid BM, Bartocci M, Basel D, Batkovskytė D, Beleză-Meireles A, Conner P, et al. 2021. High diagnostic yield in skeletal ciliopathies using massively parallel genome sequencing, structural variant screening and RNA analyses. *J Hum Genet* **66**: 995–1008. doi:10.1038/s10038-021-00925-x
- Huber C, Cormier-Daire V. 2012. Ciliary disorder of the skeleton. *Am J Med Genet C Semin Med Genet* **160C**: 165–174. doi:10.1002/ajmg.c.31336
- Kingsmore SF, Cakici JA, Clark MM, Gaughran M, Feddock M, Batalov S, Bainbridge MN, Carroll J, Caylor SA, Clarke C, et al. 2019. A randomized, controlled trial of the analytic and diagnostic performance of singleton and trio, rapid genome and exome sequencing in ill infants. *Am J Hum Genet* **105**: 719–733. doi:10.1016/j.ajhg.2019.08.009
- Krakow D, Lachman RS, Rimoin DL. 2009. Guidelines for the prenatal diagnosis of fetal skeletal dysplasias. *Genet Med* **11**: 127–133. doi:10.1097/GIM.0b013e3181971ccb
- Lee H, Deignan JL, Dorrani N, Strom SP, Kantarci S, Quintero-Rivera F, Das K, Toy T, Harry B, Yourshaw M, et al. 2014. Clinical exome sequencing for genetic identification of rare Mendelian disorders. *J Am Med Assoc* **312**: 1880–1887. doi:10.1001/jama.2014.14604
- Malinowski J, Miller DT, Demmer L, Gannon J, Pereira EM, Schroeder MC, Scheuner MT, Tsai AC, Hickey SE, Shen J. 2020. Systematic evidence-based review: outcomes from exome and genome sequencing for pediatric patients with congenital anomalies or intellectual disability. *Genet Med* **22**: 986–1004. doi:10.1038/s41436-020-0771-z
- Maron JL, Kingsmore SF, Wigby K, Chowdhury S, Dimmock D, Poindexter B, Suhrie K, Vockley J, Diacovo T, Gelb BD, et al. 2021. Novel variant findings and challenges associated with the clinical integration of genomic testing: an interim report of the genomic medicine for ill neonates and infants (GEMINI) study. *JAMA Pediatr* **175**: e205906. doi:10.1001/jamapediatrics.2020.5906
- Merrill AE, Merriman B, Farrington-Rock C, Camacho N, Sebald ET, Funari VA, Schibler MJ, Firestein MH, Cohn ZA, Priore MA, et al. 2009. Ciliary abnormalities due to defects in the retrograde transport protein *DYNC2H1* in short-rib polydactyly syndrome. *Am J Hum Genet* **84**: 542–549. doi:10.1016/j.ajhg.2009.03.015
- Murdock DR, Dai H, Burrage LC, Rosenfeld JA, Ketkar S, Müller MF, Yépez VA, Gagneur J, Liu P, Chen S, et al. 2021. Transcriptome-directed analysis for Mendelian disease diagnosis overcomes limitations of conventional genomic testing. *J Clin Invest* **131**: e141500. doi:10.1172/JCI141500
- Rentas S, Rath KS, Kaur M, Raman P, Krantz ID, Sarmady M, Tayoun AA. 2020. Diagnosing Cornelia de Lange syndrome and related neurodevelopmental disorders using RNA sequencing. *Genet Med* **22**: 927–936. doi:10.1038/s41436-019-0741-5
- Richards S, Aziz N, Bale S, Bick D, Das S, Gastier-Foster J, Grody WW, Hegde M, Lyon E, Spector E, et al. 2015. Standards and guidelines for the interpretation of sequence variants: a joint consensus recommendation of the American College of Medical Genetics and Genomics and the Association for Molecular Pathology. *Genet Med* **17**: 405–424. doi:10.1038/gim.2015.30
- Roberts AJ. 2018. Emerging mechanisms of dynein transport in the cytoplasm versus the cilium. *Biochem Soc Trans* **46**: 967–982. doi:10.1042/BST20170568
- Schmidts M, Mitchison HM. 2018. Severe skeletal abnormalities caused by defects in retrograde intraflagellar transport dyneins. *Dyneins* **2**: 356–401. doi:10.1016/B978-0-12-809470-9.00015-1
- Schmidts M, Arts HH, Bongers EM, Yap Z, Oud MM, Antony D, Duijkers L, Emes RD, Stalker J, Yntema JB, et al. 2013a. Exome sequencing identifies *DYNC2H1* mutations as a common cause of asphyxiating thoracic dystrophy (Jeune syndrome) without major polydactyly, renal or retinal involvement. *J Med Genet* **50**: 309–323. doi:10.1136/jmedgenet-2012-101284
- Schmidts M, Vodopiutz J, Christou-Savina S, Cortés CR, McInerney-Leo AM, Emes RD, Arts HH, Tüysüz B, D’Silva J, Leo PJ, et al. 2013b. Mutations in the gene encoding IFT dynein complex component *WDR34* cause Jeune asphyxiating thoracic dystrophy. *Am J Hum Genet* **93**: 932–944. doi:10.1016/j.ajhg.2013.10.003
- Stark Z, Dashnow H, Lunke S, Tan TY, Yeung A, Sadedin S, Thorne N, Macciocca I, Gaff C, Melbourne Genomics Health Alliance, et al. 2017. A clinically driven variant prioritization framework outperforms purely computational approaches for the diagnostic analysis of singleton WES data. *Eur J Hum Genet* **25**: 1268–1272. doi:10.1038/ejhg.2017.123
- Tavanez JP, Madl T, Kooshapur H, Sattler M, Valcárcel J. 2012. hnRNP A1 proofreads 3' splice site recognition by U2AF. *Mol Cell* **45**: 314–329. doi:10.1016/j.molcel.2011.11.033
- Wieringa B, Hofer E, Weissmann C. 1984. A minimal intron length but no specific internal sequence is required for splicing the large rabbit β -globin intron. *Cell* **37**: 915–925. doi:10.1016/0092-8674(84)90426-4
- Yépez VA, Gusic M, Kopajtich R, Mertes C, Smith NH, Alston CL, Berutti R, Blessing H, Ciara E, Fang F, et al. 2021. Clinical implementation of RNA sequencing for Mendelian disease diagnostics. *Genome Med* **14**: 38. doi:10.1186/s13073-022-01019-9